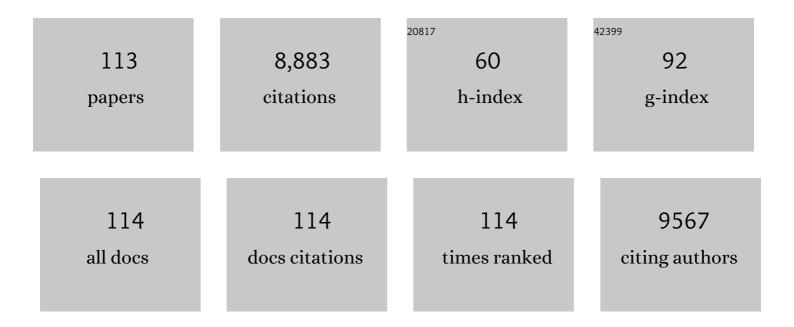
Jinming Luo

List of Publications by Year in descending order

Source: https://exaly.com/author-pdf/1772295/publications.pdf Version: 2024-02-01



#	Article	IF	CITATIONS
1	A Neural-Network-Based Optimal Resource Allocation Method for Secure IIoT Network. IEEE Internet of Things Journal, 2022, 9, 2538-2544.	8.7	28
2	Al Based Energy Efficient Routing Protocol for Intelligent Transportation System. IEEE Transactions on Intelligent Transportation Systems, 2022, 23, 1670-1679.	8.0	46
3	Improvement on the Catalytic Performance of MoO3 Nanobelts for NH3-SCR Reaction by SnO2-Modification: Enhancement of Acidity and Redox Property. Catalysis Letters, 2022, 152, 480-488.	2.6	4
4	Implanted-Electron-hydrogen boosted breaking of W O bonds to generate crater/oxygen vacancy filled WO3 nanoflakes for efficient oxidation of emerging pollutant. Journal of Alloys and Compounds, 2022, 890, 161831.	5.5	12
5	Superselective Hg(II) Removal from Water Using a Thiol-Laced MOF-Based Sponge Monolith: Performance and Mechanism. Environmental Science & Technology, 2022, 56, 2677-2688.	10.0	62
6	Zeolitic imidazolate framework-8 for ratiometric fluorescence sensing tetracyclines in environmental water based on AIE effects. Analytica Chimica Acta, 2022, 1199, 339576.	5.4	26
7	High-throughput lateral and basal interface in CeO2@Ti3C2TX: Reverse and synergistic migration of carrier for enhanced photocatalytic CO2 reduction. Journal of Colloid and Interface Science, 2022, 615, 716-724.	9.4	11
8	Ultrastable MOF-based foams for versatile applications. Nano Research, 2022, 15, 2961-2970.	10.4	20
9	Numerical Prediction of Duality Principle with Bloch-Floquet Periodic Boundary Condition in Fully Anisotropic FDTD. Remote Sensing, 2022, 14, 1135.	4.0	1
10	Effect of Presence versus Absence of Hypertension on Admission Heart Rate-Associated Cardiovascular Risk in Patients with Acute Coronary Syndrome. International Journal of Hypertension, 2022, 2022, 1-7.	1.3	2
11	Double-Network Hydrogel: A Potential Practical Adsorbent for Critical Metals Extraction and Recovery from Water. Environmental Science & amp; Technology, 2022, 56, 4715-4717.	10.0	12
12	Systematic understanding of char-volatile evolution and interaction mechanism during sewage sludge pyrolysis through in-situ tracking solid-state reaction and products fate. Journal of Hazardous Materials, 2022, 432, 128669.	12.4	8
13	Construction of metal-organic framework/polymer beads for efficient lead ions removal from water: Experiment studies and full-scale performance prediction. Chemosphere, 2022, 303, 135084.	8.2	8
14	Macro-structuring Uniform Metal–Organic Framework-Based Beads for Superselective Removal of Hg(II) from Water: Performance and Modeling. ACS ES&T Engineering, 2022, 2, 1544-1555.	7.6	4
15	Radix Astragali residue-derived porous amino-laced double-network hydrogel for efficient Pb(II) removal: Performance and modeling. Journal of Hazardous Materials, 2022, 438, 129418.	12.4	14
16	Hierarchical Ag3PO4@ZnIn2S4 nanoscoparium: An innovative Z-scheme photocatalyst for highly efficient and predictable tetracycline degradation. Journal of Colloid and Interface Science, 2021, 586, 708-718.	9.4	105
17	Atomicâ€Level and Modulated Interfaces of Photocatalyst Heterostructure Constructed by External Defectâ€Induced Strategy: A Critical Review. Small, 2021, 17, e2004980.	10.0	63
18	Comparative toxicity reduction potential of UV/sodium percarbonate and UV/hydrogen peroxide treatments for bisphenol A in water: An integrated analysis using chemical, computational, biological, and metabolomic approaches. Water Research, 2021, 190, 116755.	11.3	37

#	Article	IF	CITATIONS
19	Efficient electrochemical dehalogenation of florfenicol without discharging toxic intermediates via direct electron transfer over electrochromic WO3. Chemical Engineering Journal, 2021, 412, 127481.	12.7	24
20	Review of Advances in Engineering Nanomaterial Adsorbents for Metal Removal and Recovery from Water: Synthesis and Microstructure Impacts. ACS ES&T Engineering, 2021, 1, 623-661.	7.6	61
21	Critical Review of Advances in Engineering Nanomaterial Adsorbents for Metal Removal and Recovery from Water: Mechanism Identification and Engineering Design. Environmental Science & Technology, 2021, 55, 4287-4304.	10.0	106
22	Metastable Facet-Controlled Cu ₂ WS ₄ Single Crystals with Enhanced Adsorption Activity for Gaseous Elemental Mercury. Environmental Science & Technology, 2021, 55, 5347-5356.	10.0	20
23	Progress toward Hydrogels in Removing Heavy Metals from Water: Problems and Solutions—A Review. ACS ES&T Water, 2021, 1, 1098-1116.	4.6	33
24	Energy-Efficient Resource Allocation Strategy in Massive IoT for Industrial 6G Applications. IEEE Internet of Things Journal, 2021, 8, 5194-5201.	8.7	57
25	Research on Electromagnetic Wave Propagation Characteristics of Fully Ionized Inhomogeneous Dusty Plasma in a Magnetized BGK Model. IEEE Transactions on Plasma Science, 2021, 49, 1460-1467.	1.3	8
26	Isolation and identification of the bitter compound from Huangjiu. Food Chemistry, 2021, 349, 129133.	8.2	17
27	Gradient Hydrogen Migration Modulated with Self-Adapting S Vacancy in Copper-Doped ZnIn ₂ S ₄ Nanosheet for Photocatalytic Hydrogen Evolution. ACS Nano, 2021, 15, 15238-15248.	14.6	173
28	Highly Efficient and Selective Hg(II) Removal from Water Using Multilayered Ti ₃ C ₂ O <i>_x</i> MXene via Adsorption Coupled with Catalytic Reduction Mechanism. Environmental Science & Technology, 2020, 54, 16212-16220.	10.0	92
29	Development of a highly efficient electrochemical flow-through anode based on inner in-site enhanced TiO2-nanotubes array. Environment International, 2020, 140, 105813.	10.0	40
30	Three-dimensional electrode interface assembled from rGO nanosheets and carbon nanotubes for highly electrocatalytic oxygen reduction. Chemical Engineering Journal, 2019, 378, 122127.	12.7	32
31	A Critical Review on Energy Conversion and Environmental Remediation of Photocatalysts with Remodeling Crystal Lattice, Surface, and Interface. ACS Nano, 2019, 13, 9811-9840.	14.6	331
32	Development of a Three-Dimensional Electrochemical System Using a Blue TiO ₂ /SnO ₂ à€"Sb ₂ O ₃ Anode for Treating Low-Ionic-Strength Wastewater. Environmental Science & Technology, 2019, 53, 13784-13793.	10.0	45
33	Nanomaterial Adsorbent Design: From Bench Scale Tests to Engineering Design. Environmental Science & Technology, 2019, 53, 10537-10538.	10.0	33
34	Deep Dehalogenation of Florfenicol Using Crystalline CoP Nanosheet Arrays on a Ti Plate via Direct Cathodic Reduction and Atomic H. Environmental Science & Technology, 2019, 53, 11932-11940.	10.0	67
35	Phase-Mediated Heavy Metal Adsorption from Aqueous Solutions Using Two-Dimensional Layered MoS ₂ . ACS Applied Materials & Interfaces, 2019, 11, 38789-38797.	8.0	82
36	Heterogeneous degradation of carbamazepine by Prussian blue analogues in the interlayers of layered double hydroxides: performance, mechanism and toxicity evaluation. Journal of Materials Chemistry A, 2019, 7, 342-352.	10.3	67

#	Article	IF	CITATIONS
37	Tuning Pb(II) Adsorption from Aqueous Solutions on Ultrathin Iron Oxychloride (FeOCI) Nanosheets. Environmental Science & Technology, 2019, 53, 2075-2085.	10.0	121
38	Carbon quantum dot-sensitized and tunable luminescence of Ca ₁₉ Mg ₂ (PO ₄) ₁₄ :Ln ³⁺ (Ln ³⁺ =) Tj <u>F</u> TQq0	0 QrgBT /Ov
	<i>via</i> a sol–gel process. Journal of Materials Chemistry C, 2019, 7, 2361-2375.		
39	One–step reductive synthesis of Ti3+ self–doped elongated anatase TiO2 nanowires combined with reduced graphene oxide for adsorbing and degrading waste engine oil. Journal of Hazardous Materials, 2019, 378, 120752.	12.4	27
40	Deactivation Mechanism of Multipoisons in Cement Furnace Flue Gas on Selective Catalytic Reduction Catalysts. Environmental Science & 2019, Technology, 2019, 53, 6937-6944.	10.0	75
41	The individual and Co-exposure degradation of benzophenone derivatives by UV/H2O2 and UV/PDS in different water matrices. Water Research, 2019, 159, 102-110.	11.3	79
42	Oxidation Mechanisms of the UV/Free Chlorine Process: Kinetic Modeling and Quantitative Structure Activity Relationships. Environmental Science & amp; Technology, 2019, 53, 4335-4345.	10.0	70
43	Admission Heart Rate Is Associated With Coronary Artery Disease Severity and Complexity in Patients With Acute Coronary Syndrome. Angiology, 2019, 70, 774-781.	1.8	2
44	Sea-urchin-structure g-C3N4 with narrow bandgap (˜2.0 eV) for efficient overall water splitting under visible light irradiation. Applied Catalysis B: Environmental, 2019, 249, 275-281.	20.2	110
45	3D hierarchical porous-structured biochar aerogel for rapid and efficient phenicol antibiotics removal from water. Chemical Engineering Journal, 2019, 368, 639-648.	12.7	124
46	Electrochemical Pretreatment for Sludge Sulfide Control without Chemical Dosing: A Mechanistic Study. Environmental Science & Technology, 2019, 53, 14559-14567.	10.0	17
47	Ultrafine palladium nanoparticles supported on 3D self-supported Ni foam for cathodic dechlorination of florfenicol. Chemical Engineering Journal, 2019, 359, 894-901.	12.7	136
48	Sulfadiazine destruction by chlorination in a pilot-scale water distribution system: Kinetics, pathway, and bacterial community structure. Journal of Hazardous Materials, 2019, 366, 88-97.	12.4	61
49	Electrochemical oxidation and advanced oxidation processes using a 3D hexagonal Co3O4 array anode for 4-nitrophenol decomposition coupled with simultaneous CO2 conversion to liquid fuels via a flower-like CuO cathode. Water Research, 2019, 150, 330-339.	11.3	147
50	Oxidation of Microcystin-LR via Activation of Peroxymonosulfate Using Ascorbic Acid: Kinetic Modeling and Toxicity Assessment. Environmental Science & Technology, 2018, 52, 4305-4312.	10.0	114
51	Difference in anisotropic etching characteristics of alkaline and copper based acid solutions for single-crystalline Si. Scientific Reports, 2018, 8, 3408.	3.3	39
52	New insight on the adsorption capacity of metallogels for antimonite and antimonate removal: From experimental to theoretical study. Journal of Hazardous Materials, 2018, 346, 218-225.	12.4	35
53	Degradation of dyes by peroxymonosulfate activated by ternary CoFeNi-layered double hydroxide: Catalytic performance, mechanism and kinetic modeling. Journal of Colloid and Interface Science, 2018, 515, 92-100.	9.4	92
54	Efficient heavy metal removal from industrial melting effluent using fixed-bed process based on porous hydrogel adsorbents. Water Research, 2018, 131, 246-254.	11.3	291

#	Article	IF	CITATIONS
55	Oxidation of cefalexin by thermally activated persulfate: Kinetics, products, and antibacterial activity change. Journal of Hazardous Materials, 2018, 354, 153-160.	12.4	74
56	Highly Selective Adsorption of Antimonite by Novel Imprinted Polymer with Microdomain Confinement Effect. Journal of Chemical & Engineering Data, 2018, 63, 1513-1523.	1.9	12
57	Sodium dodecyl sulfate intercalated and acrylamide anchored layered double hydroxides: A multifunctional adsorbent for highly efficient removal of Congo red. Journal of Colloid and Interface Science, 2018, 521, 172-182.	9.4	78
58	Synthesis and characterizations of metal-free Semiconductor/MOFs with good stability and high photocatalytic activity for H2 evolution: A novel Z-Scheme heterostructured photocatalyst formed by covalent bonds. Applied Catalysis B: Environmental, 2018, 220, 607-614.	20.2	209
59	Arsenic adsorption on α-MnO2 nanofibers and the significance of (1 0 0) facet as compared with (1 1 0). Chemical Engineering Journal, 2018, 331, 492-500.	12.7	106
60	Mechanism investigation of anoxic Cr(VI) removal by nano zero-valent iron based on XPS analysis in time scale. Chemical Engineering Journal, 2018, 335, 945-953.	12.7	174
61	The role of reactive oxygen species and carbonate radical in oxcarbazepine degradation via UV, UV/H2O2: Kinetics, mechanisms and toxicity evaluation. Water Research, 2018, 147, 204-213.	11.3	103
62	Pb(<scp>ii</scp>), Cu(<scp>ii</scp>) and Cd(<scp>ii</scp>) removal using a humic substance-based double network hydrogel in individual and multicomponent systems. Journal of Materials Chemistry A, 2018, 6, 20110-20120.	10.3	106
63	TiO2 Nanotubes/Ag/MoS2 Meshy Photoelectrode with Excellent Photoelectrocatalytic Degradation Activity for Tetracycline Hydrochloride. Nanomaterials, 2018, 8, 666.	4.1	15
64	Impact of Chloride Ions on UV/H ₂ O ₂ and UV/Persulfate Advanced Oxidation Processes. Environmental Science & amp; Technology, 2018, 52, 7380-7389.	10.0	178
65	Destruction of phenicol antibiotics using the UV/H2O2 process: Kinetics, byproducts, toxicity evaluation and trichloromethane formation potential. Chemical Engineering Journal, 2018, 351, 867-877.	12.7	66
66	Mesoporous TiO2 with WO3 functioning as dopant and light-sensitizer: A highly efficient photocatalyst for degradation of organic compound. Journal of Hazardous Materials, 2018, 358, 44-52.	12.4	41
67	Electrocatalytic dechlorination of halogenated antibiotics via synergistic effect of chlorine-cobalt bond and atomic H*. Journal of Hazardous Materials, 2018, 358, 294-301.	12.4	44
68	Lithium ion-imprinted polymers with hydrophilic PHEMA polymer brushes: The role of grafting density in anti-interference and anti-blockage in wastewater. Journal of Colloid and Interface Science, 2017, 492, 146-156.	9.4	31
69	Antimony Removal from Aqueous Solution Using Novel α-MnO ₂ Nanofibers: Equilibrium, Kinetic, and Density Functional Theory Studies. ACS Sustainable Chemistry and Engineering, 2017, 5, 2255-2264.	6.7	85
70	Selective removal Pb(<scp>ii</scp>) ions form wastewater using Pb(<scp>ii</scp>) ion-imprinted polymers with bi-component polymer brushes. RSC Advances, 2017, 7, 25811-25820.	3.6	26
71	Photocatalytic wastewater purification with simultaneous hydrogen production using MoS 2 QD-decorated hierarchical assembly of ZnIn 2 S 4 on reduced graphene oxide photocatalyst. Water Research, 2017, 121, 11-19.	11.3	176
72	Selfâ€Optimization of the Active Site of Molybdenum Disulfide by an Irreversible Phase Transition during Photocatalytic Hydrogen Evolution. Angewandte Chemie - International Edition, 2017, 56, 7610-7614.	13.8	221

#	Article	IF	CITATIONS
73	Selfâ€Optimization of the Active Site of Molybdenum Disulfide by an Irreversible Phase Transition during Photocatalytic Hydrogen Evolution. Angewandte Chemie, 2017, 129, 7718-7722.	2.0	61
74	Microbial mediated arsenic biotransformation in wetlands. Frontiers of Environmental Science and Engineering, 2017, 11, 1.	6.0	67
75	Micro-structured inverted pyramid texturization of Si inspired by self-assembled Cu nanoparticles. Nanoscale, 2017, 9, 907-914.	5.6	59
76	The preparation and performance of lignin-based activated carbon fiber adsorbents for treating gaseous streams. Frontiers of Chemical Science and Engineering, 2017, 11, 328-337.	4.4	32
77	Enhancement of Phosphate Adsorption on Zirconium Hydroxide by Ammonium Modification. Industrial & Engineering Chemistry Research, 2017, 56, 9419-9428.	3.7	48
78	Phosphor-Doped Thermal Barrier Coatings Deposited by Air Plasma Spray for In-Depth Temperature Sensing. Sensors, 2016, 16, 1490.	3.8	8
79	Three-Dimensional Reduced Graphene Oxide Coupled with Mn ₃ O ₄ for Highly Efficient Removal of Sb(III) and Sb(V) from Water. ACS Applied Materials & Interfaces, 2016, 8, 18140-18149.	8.0	120
80	Zirconia (ZrO ₂) Embedded in Carbon Nanowires via Electrospinning for Efficient Arsenic Removal from Water Combined with DFT Studies. ACS Applied Materials & Interfaces, 2016, 8, 18912-18921.	8.0	83
81	Surface Tuning of La _{0.5} Sr _{0.5} CoO ₃ Perovskite Catalysts by Acetic Acid for NO _{<i>x</i>} Storage and Reduction. Environmental Science & amp; Technology, 2016, 50, 6442-6448.	10.0	108
82	Synthesis and efficient visible light photocatalytic H2 evolution of a metal-free g-C3N4/graphene quantum dots hybrid photocatalyst. Applied Catalysis B: Environmental, 2016, 193, 103-109.	20.2	218
83	A Strategy for One-Pot Conversion of Organic Pollutants into Useful Hydrocarbons through Coupling Photodegradation of MB with Photoreduction of CO ₂ . ACS Catalysis, 2016, 6, 6861-6867.	11.2	128
84	Capturing Lithium from Wastewater Using a Fixed Bed Packed with 3-D MnO ₂ Ion Cages. Environmental Science & Technology, 2016, 50, 13002-13012.	10.0	102
85	Women With Early Menopause Have Higher Rates of Target Lesion Revascularization After Percutaneous Coronary Intervention. Angiology, 2016, 67, 311-316.	1.8	1
86	A highly efficient polyampholyte hydrogel sorbent based fixed-bed process for heavy metal removal in actual industrial effluent. Water Research, 2016, 89, 151-160.	11.3	213
87	Interface Engineering of High Efficiency Organic-Silicon Heterojunction Solar Cells. ACS Applied Materials & amp; Interfaces, 2016, 8, 26-30.	8.0	35
88	Comparison of MoO3 and WO3 on arsenic poisoning V2O5/TiO2 catalyst: DRIFTS and DFT study. Applied Catalysis B: Environmental, 2016, 181, 692-698.	20.2	117
89	Insulin Resistance Increases the Risk of Contrast-Induced Nephropathy in Patients Undergoing Elective Coronary Intervention. Angiology, 2016, 67, 139-145.	1.8	13
90	Maskless inverted pyramid texturization of silicon. Scientific Reports, 2015, 5, 10843.	3.3	87

#	Article	IF	CITATIONS
91	Fabrication of novel heterostructured few layered WS2-Bi2WO6/Bi3.84W0.16O6.24 composites with enhanced photocatalytic performance. Applied Catalysis B: Environmental, 2015, 179, 220-228.	20.2	78
92	Hierarchically mesostructured MIL-101 metal–organic frameworks with different mineralizing agents for adsorptive removal of methyl orange and methylene blue from aqueous solution. Journal of Environmental Chemical Engineering, 2015, 3, 1372-1383.	6.7	77
93	Ceria promotion on the potassium resistance of MnOx/TiO2 SCR catalysts: An experimental and DFT study. Chemical Engineering Journal, 2015, 269, 44-50.	12.7	92
94	Recovery of Lithium from Wastewater Using Development of Li Ion-Imprinted Polymers. ACS Sustainable Chemistry and Engineering, 2015, 3, 460-467.	6.7	133
95	Synthesis of graphene oxide/schwertmannite nanocomposites and their application in Sb(V) adsorption from water. Chemical Engineering Journal, 2015, 270, 205-214.	12.7	98
96	Adsorptive Removal of Pb(II) Ions from Aqueous Samples with Amino-Functionalization of Metal–Organic Frameworks MIL-101(Cr). Journal of Chemical & Engineering Data, 2015, 60, 1732-1743.	1.9	172
97	Fabrication and Electrochemical Treatment Application of an Al-Doped PbO ₂ Electrode with High Oxidation Capability, Oxygen Evolution Potential and Reusability. Journal of the Electrochemical Society, 2015, 162, E258-E262.	2.9	30
98	Removal of Cadmium(II) from Wastewater Using Novel Cadmium Ion-Imprinted Polymers. Journal of Chemical & Engineering Data, 2015, 60, 3253-3261.	1.9	66
99	Removal of Antimonite (Sb(III)) and Antimonate (Sb(V)) from Aqueous Solution Using Carbon Nanofibers That Are Decorated with Zirconium Oxide (ZrO ₂). Environmental Science & Technology, 2015, 49, 11115-11124.	10.0	233
100	Deactivation and regeneration of a commercial SCR catalyst: Comparison with alkali metals and arsenic. Applied Catalysis B: Environmental, 2015, 168-169, 195-202.	20.2	180
101	Hydrogen Evolution from Water Coupled with the Oxidation of As(III) in a Photocatalytic System. ACS Applied Materials & Interfaces, 2015, 7, 28429-28437.	8.0	9
102	Metagenomic Approach Reveals Variation of Microbes with Arsenic and Antimony Metabolism Genes from Highly Contaminated Soil. PLoS ONE, 2014, 9, e108185.	2.5	75
103	Insight into Deactivation of Commercial SCR Catalyst by Arsenic: An Experiment and DFT Study. Environmental Science & Technology, 2014, 48, 13895-13900.	10.0	98
104	Optimization of silicon pyramidal emitter by self-selective Ag-assisted chemical etching. RSC Advances, 2014, 4, 24458.	3.6	12
105	Preparation of waterâ€compatible molecularly imprinted polymers for caffeine with a novel ionic liquid as a functional monomer. Journal of Applied Polymer Science, 2013, 127, 2884-2890.	2.6	33
106	Grafting of molecularly imprinted polymers from the surface of Fe ₃ O ₄ nanoparticles containing double bond via suspension polymerization in aqueous environment: A selective sorbent for theophylline. Journal of Applied Polymer Science, 2011, 121, 1930-1937.	2.6	21
107	Photocatalytic reduction of Cr(VI) on WO3 doped long TiO2 nanotube arrays in the presence of citric acid. Applied Catalysis B: Environmental, 2010, 94, 142-149.	20.2	227
108	High Efficient Photocatalytic Degradation of p-Nitrophenol on a Unique Cu ₂ 0/TiO ₂ p-n Heterojunction Network Catalyst. Environmental Science & Technology, 2010, 44, 7641-7646.	10.0	448

Jinming Luo

#	Article	IF	CITATIONS
109	Fabrication of CdSe Nanoparticles Sensitized Long TiO ₂ Nanotube Arrays for Photocatalytic Degradation of Anthracene-9-carbonxylic Acid under Green Monochromatic Light. Journal of Physical Chemistry C, 2010, 114, 4783-4789.	3.1	89
110	Sensitive Detection of Polycyclic Aromatic Hydrocarbons Using CdTe Quantum Dot-Modified TiO ₂ Nanotube Array through Fluorescence Resonance Energy Transfer. Environmental Science & Technology, 2010, 44, 7884-7889.	10.0	63
111	Biosorption of cadmium(II) from aqueous solutions by industrial fungus Rhizopus cohnii. Transactions of Nonferrous Metals Society of China, 2010, 20, 1104-1111.	4.2	58
112	Carbon-Nanotube-Guiding Oriented Growth of Gold Shrubs on TiO ₂ Nanotube Arrays. Journal of Physical Chemistry C, 2010, 114, 7694-7699.	3.1	20
113	Analysis of Gaussian beam broadening and scintillation index in anisotropic plasma turbulence. Waves in Random and Complex Media, 0, , 1-16.	2.7	6